Malaysian Journal of Science **26** (SKSM14 Special Issue): 53 - 64 (2007)

A Numerical Solution of Wave Motion in Viscoelastic Rods (Standard Linear Solid Model)

Abu Bakar Musa

Department of Engineering Science and Mathematics, College of Engineering, University Tenaga Nasional, Malaysia.
bakar@uniten.edu.my

ABSTRACT This study is about the propagation of waves through a short rod (or slug) of viscoelastic material. The viscoelastic material are modelled as standard linear solids which involve three material parameters and the motion is treated as one-dimensional. In this study, a viscoelastic slug is placed between two semi-infinite elastic rods and a wave initiated in the first rod is transmitted through the slug into the second rod. The objective is to relate the transmitted signal to the material parameters of the slug. We solve the governing system of partial differential equations using Laplace transform. We invert the Laplace transformed solution numerically to obtain the transmitted signal for several viscosity time constants and ratios of acoustic impedances. In inverting the Laplace transformed equations, we used the complex inversion formula because there is a branch cut and infinitely many poles within the Bromwich contour. Finally, we discuss the relationship between the viscosity time constants, ratios of acoustic impedances and the results of the interface velocity discontinuities.

ABSTRAK Kajian ini mengkaji pergerakan gelombang yang melalui satu batang bahan yang anjal-likat dan pendek. Batang anjal-likat yang pendek tersebut dimodelkan melibatkan 3 bahan parameter dan pergerakan gelombang di dalamnya dikira sebagai satu dimensi. Dalam kajian ini, batang pendek yang anjal-likat tersebut ditempatkan di antara dua batang anjal yang mempunyai ukuran panjang yang tak terhingga. Kemudian satu gelombang diterbitkan di dalam batang anjal yang pertama dan gelombang tersebut bergerak dan menembusi batang anjal-likat yang pendek lalu terus menuju kepada batang anjal yang kedua. Tujuan kajian ini adalah untuk mengkaji hubung kait di antara gelombang yang menembusi batang anjal-likat dan parameter yang terdapat pada batang anjal-likat tersebut. Pada permulaannya kita selesai satu sistem persamaan separa dengan menggunakan penjelmaan Laplace. Kemudian kita songsangkan persamaan jelmaan Laplace secara berangka untuk mendapatkan ukuran gelombang yang menembusi batang anjal-likat tersebut bagi beberapa parameter kelikatan serta nisbah galangan akustik. Untuk mendapatkan songsangan jelmaan Laplace, kita perlu menggunakan formula songsang kompleks kerana terdapat satu "potongan cabang"(branch cut) dan punca dengan jumlah tak terhingga di dalam kontor Bromwich. Akhir sekali kita bincangkan hubung kait di antara parameter kelikatan, nisbah galangan akustik dan hasilan dari pengiraan berangka bagi kelajuan gelombang yang terputus pada permukaan.

(interface velocity discontinuity, ratio of acoustic impedances, viscosity time constants, z-effective)

INTRODUCTION

There are materials for which a suddenly applied and maintained state of uniform stress induces an instantaneous deformation followed by a flow process which may or may not be limited in magnitude as time grows [1]. These materials are said to exhibit both an instantaneous elasticity effect and a creep characteristic. This behavior clearly cannot be described by either elasticity or viscosity theories alone as it combines features of each and is called viscoelastic. Viscoelasticity is a generalization of elasticity and viscosity. The

ideal linear elastic element is the spring whilst the ideal linear viscous element is the dashpot. Energy is stored in springs as elastic strain energy and energy is dissipated in a dashpot as heat [2]. This paper deals with the transmission of waves through a viscoelastic material which is modeled by a small rod (slug) of the material placed between two semi-infinite elastic rods. The purpose of this paper is to determine the properties of the viscoelastic slug after a wave initiated in the first semi-infinite elastic rod is transmitted through the viscoelastic slug into the semi-infinite elastic rod.

There are three different types of vibration which occur in thin rods or bars namely longitudinal, torsional and lateral. In longitudinal vibrations, elements of the rod extend and contract whereas in torsional vibrations, each transverse section of the rod remains in its own plane and rotates about its centre, the axis of the rod remaining undisturbed. Lateral vibrations refer to the flexure of portions of the rod, elements of the central axis moving laterally during the motion [3]. The velocities proportion of all these elastic waves depend, amongst other factors, on the elastic constants and density of the solid, so that the dynamic elastic constants can be determined from the velocity of propagation [3]. When the solid is not perfectly elastic then some of the energy of the stress wave dissipate as it goes through the medium, so the strength of the stress wave attenuates as it travels through the medium. In this paper, we consider each plane cross-section of the rod to remain plane during the motion and the stress over it to be uniform, so that the motion is longitudinal and one-dimensional.

In this problem, we investigate the bahaviours of the longitudinal waves after the waves transmitted through a finite length viscoelastic slug. We model the viscoelastic material as a standard linear solid (Figure 1). We model the system where a finite length viscoelastic slug is placed between two semi-infinite elastic rods as an idealization of the experimental work described by H. Kolsky [4]. Many dynamical system are so complex that analytical solutions cannot be found and numerical solution is the only answer. Here, we numerically compute the waves transmitted through the slug into the second semi-infinite elastic rod. Results are obtained for several viscosity time constants and several ratios of acoustic impedance.

MATHEMATICAL MODEL OF WAVE PROPAGATION IN VISCOELASTIC MATERIAL

In this problem, we investigate the dynamic behaviours of a viscoelastic slug which is placed between two semi-infinite elastic rods as shown in Figure 2. A velocity discontinuity wave is initiated in the first rod and propagates through the viscoelastic slug moving into the second semi-infinite elastic rod. There are multiple reflections and transmission of waves in the viscoelastic slug. When the waves arrive at the interface between the first rod and the slug, some of the waves are transmitted and some of them are reflected. The same situation happens when the waves reach the second interface between the slug and the second rod. We first obtain the governing equations and non-dimensionalise them. Secondly, we state the associated boundary conditions and non-dimensionalised them. We then solve the differential equations with prescribed boundary conditions in the Laplace transform domain.

GOVERNING EQUATIONS

Let $\breve{u}$ be the additional displacement in the first rod, and $\breve{v}$ and $\breve{w}$ be the displacements in the slug and in the rod following the wave propagation respectively, where the notation $\breve{}$ indicates dimensional variables. Let $\breve{\sigma}_v$ be the stress in the slug, $\breve{\sigma}_u$ and $\breve{\sigma}_w$ be the stress in the first rod and in the second rod respectively, $\overline{E}$ and E be young's modulus in the slug and in the rod respectively, $\overline{\rho}$ and ρ be the density in the slug and in the rods respectively. We choose the origin of coordinates at the centre of the first interface and axis $0\breve{X}$ along the axis of the slug and we assume the wave reaches the viscoelastic slug at time $\breve{t}=0$. When the wave, initiated in the first rod with constant velocity discontinuity V, reaches the slug at time $\breve{t}=0$ and $\breve{X}=0$, we can write the position at time $\breve{t}$ of the cross-section of the

first rod which was at location $\breve{X}$ at time $\breve{t}=0$ as

$$\breve{x}(\breve{X},\breve{t})=\breve{X}+V\left(\breve{t}-\frac{\breve{X}}{c}\right)H\left(\breve{t}-\frac{\breve{X}}{c}\right)+\breve{u}(\breve{X},\breve{t}) \quad \text{for } \breve{X}\le 0 \qquad (1)$$

where $H(t)$ is the Heaviside function and V is a constant. At time $\breve{t}$, the cross-section of the slug which at location $\breve{X}$ at time $\breve{t}=0$ is $\breve{x}(\breve{X},\breve{t})$ given by

$$\breve{x}(\breve{X},\breve{t})=\breve{X}+\breve{v}(\breve{X},\breve{t}) \quad \text{for} \quad 0\le\breve{X}\le h_s \qquad (2)$$

where h_s is the length of the slug. We write the position at time $\breve{t}$ of the cross-section of the second rod which at location $\breve{X}$ at time $\breve{t}=0$ as

$$\breve{x}(\breve{X},\breve{t})=\breve{X}+\breve{w}(\breve{X},\breve{t}) \quad \text{for} \quad \breve{X}\ge h. \qquad (3)$$

The stress in the body is denoted by $\breve{\sigma}(\breve{X},\breve{t})$ and at the cross-section X, the cross-sectional area is A. We focus on a small section of length $\delta\breve{X}$ in the body. Then considering the external forces in this section [3],

$$\left(\breve{\sigma}+\frac{\partial\breve{\sigma}}{\partial\breve{X}}\delta\breve{X}\right)A-\breve{\sigma}A=\rho A\frac{\partial^2\breve{u}}{\partial\breve{t}^2}\delta\breve{X} \qquad (4)$$

$$\frac{\partial\breve{\sigma}}{\partial\breve{X}}=\rho\frac{\partial^2\breve{u}}{\partial\breve{t}^2}. \qquad (5)$$

Then the equation of motion [5] in the first rod is

$$\frac{\partial\breve{\sigma}_u}{\partial\breve{X}}=\rho\frac{\partial^2\breve{u}}{\partial\breve{t}^2}, \qquad (6)$$

the equation of motion in the slug is

$$\frac{\partial\breve{\sigma}_v}{\partial\breve{X}}=\bar{\rho}\frac{\partial^2\breve{u}}{\partial\breve{t}^2} \qquad (7)$$

and the equation of motion[5] in the second rod is

$$\frac{\partial\breve{\sigma}_w}{\partial\breve{X}}=\rho\frac{\partial^2\breve{u}}{\partial\breve{t}^2}. \qquad (8)$$

We model the slug as standard linear solid so that the constitutive equation in the slug is

$$\breve{\sigma}_v+\bar{\bar{\mu}}\frac{\partial\breve{\sigma}_v}{\partial\breve{t}}=\bar{\bar{E}}\left(\frac{\partial\breve{v}}{\partial\breve{X}}+\bar{\bar{\eta}}\frac{\partial^2\breve{v}}{\partial\breve{t}\partial\breve{X}}\right) \qquad (9)$$

The stress-strain relations in the rods are

$$\breve{\sigma}_u=E\left(-\frac{V}{c}H\left(\breve{t}-\frac{\breve{X}}{c}\right)+\frac{\partial\breve{u}}{\partial\breve{X}}\right), \qquad (10)$$

$$\breve{\sigma}_w=E\frac{\partial\breve{w}}{\partial\breve{X}}. \qquad (11)$$

We now define the non-dimensional quantities $x,X,t,u,v,w,\sigma_u,\sigma_v,\sigma_w,\bar{\mu},\bar{\eta}$ by the non-dimensionalising scheme

$$\breve{X}=h_sX,\ \breve{x}=h_sx,\ \breve{t}=\frac{h_s}{c}t,$$
$$\breve{u}=\frac{V}{c}h_su,\ \breve{v}=\frac{V}{c}h_sv,\ \breve{w}=\frac{V}{c}h_sw,$$
$$\breve{\sigma}_u=E\sigma_u,\ \breve{\sigma}_v=E\sigma_v,\ \breve{\sigma}_w=E\sigma_w,$$
$$\bar{\bar{\eta}}=\frac{h_s}{\bar{c}}\bar{\eta},\ \bar{\bar{\mu}}=\frac{h_s}{\bar{c}}\bar{\mu},\ \bar{\bar{\eta}}>\bar{\bar{\mu}} \qquad (12)$$

where $c^2=\frac{E}{\rho}$, $\bar{c}^2=\frac{\bar{E}}{\bar{\rho}}$, $z=\frac{\rho c}{\bar{\rho}\bar{c}}$ and $\alpha=\frac{c}{\bar{c}}$.

If we now use (12) to non-dimensionalise equations (1), (2) and (3), we obtain

$$x=X+\frac{V}{c}(t-X)H(t-X)+\frac{V}{c}u(X,t) \quad \text{for } X<0, \qquad (13)$$

$$x=X+\frac{V}{c}\alpha v(X,t) \quad \text{for } 0\le X\le 1, \qquad (14)$$

$$x=X+\frac{V}{c}w(X,t) \quad \text{for } X>1. \qquad (15)$$

We then non-dimensionalise (6)– (11), to obtain the non-dimensional equations of motion and stress-strain relations

$$\frac{\partial\sigma_u}{\partial X}=\frac{V}{c}\frac{\partial^2u}{\partial t^2}, \qquad (16)$$

$$\frac{\partial\sigma_v}{\partial X}=\alpha_2\frac{V}{\bar{c}}\frac{\partial^2v}{\partial t^2}, \qquad (17)$$

$$\frac{\partial\sigma_w}{\partial X}=\frac{V}{c}\frac{\partial^2w}{\partial t^2}, \qquad (18)$$

$$\sigma_v+\alpha\bar{\mu}\frac{\partial\sigma_v}{\partial t}=\frac{V}{\bar{c}}\left(\frac{\partial v}{\partial X}+\alpha\bar{\eta}\frac{\partial^2v}{\partial t\partial X}\right), \qquad (19)$$

$$\sigma_u = \frac{V}{c}\left(\frac{\partial u}{\partial X} - H(t-X)\right), \qquad (20)$$

$$\sigma_w = \frac{V}{c}\frac{\partial w}{\partial X}. \qquad (21)$$

We take the Laplace transforms of the equations (16)–(21) with respect to t and solve the differential equations for the displacement transforms $\hat{u}, \hat{v}, \hat{w}$ in the s domain. We obtain

$$\hat{u}(X,s) = a(s)e^{sX}, \qquad (22)$$

$$\hat{v}(X,s) = b(s)\exp\left(\frac{-\alpha s X}{\overline{\beta}(s)}\right) + d(s)\exp\left(\frac{\alpha s X}{\overline{\beta}(s)}\right), \qquad (23)$$

$$\hat{w}(X,s) = f(s)e^{-sX} \qquad (24)$$

where $\overline{\beta}^2(s) = \dfrac{1+\alpha\overline{\eta}s}{1+\alpha\overline{\mu}s}$.

In order to find $a(s)$, $b(s)$, $d(s)$ and $f(s)$, we apply the boundary conditions described as follows:

(i) The particle velocity in the first rod is equal to the velocity in the slug at the first interface ($X = 0$).

(ii) The stresses in the first rod and in the slug at $X = 0$ are equal.

(iii) The velocities in the slug and in the second rod are equal at the second interface ($X = 1$).

(iv) The stresses in the slug and in the second rod at $X = 1$ are equal.

We obtain

$$\hat{x} - \hat{X} = -\frac{2}{s^2}\sinh(sX) + \frac{2ze^{sX}\left(e^{\frac{2\alpha s}{\overline{\beta}(s)}}\left(\overline{\beta}(s)+z\right) + \overline{\beta}(s) - z\right)}{s^2\left(e^{\frac{2\alpha s}{\overline{\beta}(s)}}\left(\overline{\beta}(s)+z\right)^2 - \left(\overline{\beta}(s)-z\right)^2\right)}, \qquad (25)$$

$$\hat{v}(X,s) = \frac{2z\left[\exp\left(\frac{\alpha s}{\overline{\beta}(s)}(2-X)\right)\left(\overline{\beta}(s)+z\right) + \left(\overline{\beta}(s)-z\right)\exp\left(\frac{\alpha s X}{\overline{\beta}(s)}\right)\right]}{\alpha s^2\left(e^{\frac{2\alpha s}{\overline{\beta}(s)}}\left(\overline{\beta}(s)+z\right)^2 - \left(\overline{\beta}(s)-z\right)^2\right)}, \qquad (26)$$

$$\hat{w}(X,s) = \frac{4z\overline{\beta}(s)\exp\left(s\left(\frac{\alpha}{\overline{\beta}(s)}+1-X\right)\right)}{s^2\left(e^{\frac{2\alpha s}{\overline{\beta}(s)}}\left(\overline{\beta}(s)+z\right)^2 + \left(\overline{\beta}(s)-z\right)^2\right)}. \qquad (27)$$

In order to determine the response of the system, we need to invert the Laplace transforms of equations (25)–(27). To find the inverse Laplace transform, we apply the complex inversion formula [6] where

$$F(t) = \frac{1}{2\pi i}\int_{\gamma-i\infty}^{\gamma+i\infty} e^{st} f(s)ds, \quad t > 0. \qquad (28)$$

If $f(s) = L\{F(t)\}$. In practice, the integral in (28) is evaluated by considering the contour integral

$$\frac{1}{2\pi i}\oint_C e^{st} f(s)ds$$

where C is the contour of Figure 3. If the arc BDEFA is represented by Γ, it follows from (28) that since $\Gamma = \sqrt{R^2 - \gamma^2}$,

$$F(t) = \lim_{R\to\infty}\frac{1}{2\pi i}\int_{\gamma-i\infty}^{\gamma+i\infty} e^{st} f(s)ds = \lim_{R\to\infty}\left[\frac{1}{2\pi i}\oint_C e^{st} f(s)ds - \frac{1}{2\pi i}\int_\Gamma e^{st} f(s)ds\right] \qquad (29)$$

THE SIGNAL TRANSMITTED THROUGH THE VISCOELASTIC SLUG

The focus of this paper is to obtain the solution in the time domain of the displacement wave propagation in the second semi-infinite elastic rod by inverting the Laplace transform for the solution (27). In order to do this we use the

complex inversion formula (29) to invert the Laplace equation (27). Firstly, we apply the Bromwich contour to lay-out the calculation of the complex integrals along the contour and determine the poles and branch points. Secondly, we find all the roots in the real and complex plane until their contribution to the solution is insignificant. In searching for the roots, we have to ensure that we do not miss out any root near the real axis since they may contribute significantly to the results. Furthermore, after determining the roots, we calculate the residues and we compute the results for several values of viscosity time constants and ratios of acoustic impedances. The equation of the wave propagation in the second rod after applying (28) to (27) is

$$w(X,t) = \frac{1}{2\pi i}\int_{\gamma-iz}^{\gamma+iz} \frac{4z\bar{\beta}(s)\exp\left(s\left(\frac{\alpha}{\bar{\beta}(s)}+1-X\right)\right)}{s^2\left(e^{\frac{2\alpha s}{\bar{\beta}(s)}}\left(\bar{\beta}(s)+z\right)^2+\left(\bar{\beta}(s)-z\right)^2\right)}ds \tag{30}$$

We consider a closed curve in the left half of the complex plane and we note that there are branch points of the integrand at $s=-\frac{1}{\alpha\bar{\mu}}$ and $s=-\frac{1}{\alpha\bar{\eta}}$ (see Figure 4). Then we make a cut along $-\frac{1}{\alpha\bar{\mu}}$ and $-\frac{1}{\alpha\bar{\eta}}$, and modify the contour in order to avoid crossing the branch cut as shown in Figure 4. We let χ be the closed contour ABCDEFGHJKLMA and Γ to be the contour BCD, DE, EF, FG, GH, HJ, JK, KL, LMA. In the closed contour χ, there are a second degree pole at $s=0$ and poles when the denominator of the integrand (30) is equal to zero. Then it follows from (30), on putting $T=\sqrt{R^2-\gamma^2}$, that

$$\begin{aligned} & w(X,t) \\ &= \lim_{R\to\infty}\frac{1}{2\pi i}\int_{\gamma-iT}^{\gamma+iT} e^{st}\hat{w}(X,s)ds \\ &= \lim_{R\to\infty}\left[\frac{1}{2\pi i}\oint_{\chi} e^{st}\hat{w}(X,s)ds \right. \\ &\qquad \left. -\frac{1}{2\pi i}\int_{\Gamma} e^{st}\hat{w}(X,s)ds\right] \\ &= \sum \text{residues..inside..}\chi - \frac{1}{2\pi i}\int_{\Gamma} e^{st}\hat{w}(X,s)ds \\ &= \sum \text{residues..inside..}\chi - \int_{BCD} \\ &\quad -\int_{DE}-\int_{EF}-\int_{FG}-\int_{GH}-\int_{HJ}-\int_{JK}-\int_{KL}-\int_{LMA} \end{aligned} \tag{31}$$

In finding the roots, we used Maple software routine which required us to specify the vertices of a rectangle within which a root is located. We found 150 poles in the upper half plane and consequently their complex conjugates. This gave 300 poles in total which gives reasonably accurate results.

The residue of the second order pole at $s=0$

$$\begin{aligned} & \lim_{s\to 0}\frac{d}{ds}\left[\frac{4z\bar{\beta}(s)\exp\left(s\left(\frac{\alpha}{\bar{\beta}(s)}+1-X+t\right)\right)}{\left(e^{\frac{2\alpha s}{\bar{\beta}(s)}}\left(\bar{\beta}(s)+z\right)^2+\left(\bar{\beta}(s)-z\right)^2\right)}\right] \\ &= \frac{1}{2z}\left[2z\left(\frac{\alpha(\bar{\eta}-\bar{\mu})}{2}+2-X+t\right)\right. \\ &\qquad \left. -\alpha(1-z)^2-\alpha z(\bar{\eta}-\bar{\mu})\right]. \end{aligned} \tag{32}$$

In calculating the other residues we use

$$\text{Residue} = \lim_{s\to s_n}\frac{(s-s_n)N(s_n)}{s^2D(s)} \tag{33}$$

where $N(s) = 4z\bar{\beta}(s)\exp\left(s\left(\frac{\alpha}{\bar{\beta}(s)}+1-X+t\right)\right)$,

$D(s) = \left(e^{\frac{2\alpha s}{\bar{\beta}(s)}}\left(\bar{\beta}(s)+z\right)^2+\left(\bar{\beta}(s)-z\right)^2\right)$ and s_n is the nth root.

RESULTS

Having found the required numbers of poles to evaluate the displacement of the wave in the second rod, we obtain the displacement in the time domain

$$w(X,t) = \frac{\alpha(\bar{\eta}-\bar{\mu})}{2}+2-X+t-\frac{\alpha(1-z)^2}{2z}-\frac{\alpha z(\bar{\eta}-\bar{\mu})}{2z} + \sum \text{residue inside } \chi \qquad (34)$$

In order to get the velocity, we differentiate (34) and we run the program for several viscosity time constants and ratios of acoustic impedances. In non-dimensional time, it takes $\alpha\sqrt{\frac{\bar{\mu}}{\bar{\eta}}}$ time units for the first wave to reach the second interface between the slug and the second rod. Then a portion of the wave is transmitted into the second rod and another portion is reflected into the slug. The wave which is reflected at $X=1$ will travel back to the first interface at $X=0$. A portion of the wave is the transmitted into the first rod and another portion of the wave is reflected into the slug at non-dimensional time $2\alpha\sqrt{\frac{\bar{\mu}}{\bar{\eta}}}$. This reflected wave reaches the second interface at unit time $3\alpha\sqrt{\frac{\bar{\mu}}{\bar{\eta}}}$. The wave keeps on bouncing back and forward in the viscoelastic slug which creates multiple reflections and transmissions at both interfaces until they dies-out. In this simulation we choose the ratio of acoustics impedances, z as small as $z=0.333$ and increase it up to $z=2.0$ for viscosity parameters ratio $\frac{\bar{\eta}}{\bar{\mu}}=2$ and for the viscosity parameters ratio, $\frac{\bar{\eta}}{\bar{\mu}}=5$, from $z=0.333$ to $z=3.0$. In choosing the ratio of acoustics impedances, we also take into account the values of z for which the z effective [7], $z\sqrt{\frac{\bar{\mu}}{\bar{\eta}}}>1$. Figures 5-10 show some of the results for the particle velocity in the second rod at the interface $X=1$ with several viscosity time constants and ratios of acoustic impedances z. This is the signal which propagates in the second rod and can be employed to determine the parameters of the slug.

In all the results in Figures 5-10, the predicted velocity discontinuities at $X=1$, $t=\sqrt{\frac{\bar{\mu}}{\bar{\eta}}}$ and $t=3\sqrt{\frac{\bar{\mu}}{\bar{\eta}}}$ obtained by Musa [8] in viscoelastic discontinuity analysis agree very well with the results. The predicted velocity discontinuities obtained using viscoelastic discontinuity analysis are shown in table 1. The results also concur well with the results obtained using perturbation techniques [9] by Musa [7] for several viscosity time constants $\bar{\eta}$ and $\bar{\mu}$ and ratio of acoustic impedances, z.

DISCUSSION

For smaller viscosity time constants such as $\bar{\eta}=0.2$, $\bar{\eta}=0.5$ and $\bar{\mu}=0.1$, the initial discontinuity is small and the velocity subsequently increases smoothly and asymptotically approaches 1. As the viscosity time constants increase to $\bar{\mu}=1$ with $\bar{\eta}=2$ and $\bar{\eta}=5$, the initial discontinuity is significantly bigger and the velocity increases linearly until the second wave arrives at $t=3\alpha\sqrt{\frac{\bar{\mu}}{\bar{\eta}}}$ and the third wave arrives at $t=5\alpha\sqrt{\frac{\bar{\mu}}{\bar{\eta}}}$. For $\bar{\eta}=20$, $\bar{\eta}=50$ and $\bar{\mu}=10$, the initial jump is bigger still and the velocity remains virtually constant until the arrival of the second and subsequent jumps. The results also

show that the first jump at $X = 1$ increases as the ratio of acoustic impedances, z increases until the z effective, $z\sqrt{\frac{\overline{\mu}}{\overline{\eta}}} = 1$. As the z effective $z\sqrt{\frac{\overline{\mu}}{\overline{\eta}}}$ approaches 1, the graph shows no jumps after the first jump. Then the jumps appear again for values of z effective, $z\sqrt{\frac{\overline{\mu}}{\overline{\eta}}} > 1$. This trend is also shown in Figure 11 for viscosity parameters $\overline{\eta} = 20$ and $\overline{\mu} = 10$. At the interface $X = 1$ and $t = \alpha\sqrt{\frac{\overline{\mu}}{\overline{\eta}}}$, where the first jump occurs, the red curve shows the jump for $z = 0.333$ is 0.6062 and as z increases to $z = 667$, the discontinuity is 0.8558 and it is shown by the green curve. Furthermore as we increase z, to $z = 0.9$ the first discontinuity is 0.934 and as shown by the black curve and for $z = 1.2$, the first discontinuity is 0.9759 as shown by the blue curve in Figure 11. As z effective, $z\sqrt{\frac{\overline{\mu}}{\overline{\eta}}}$ approaches 1, as shown by the yellow curve when $z = 1.5$, the first discontinuity is 0.9816. As z goes beyond the z effective, the value of the first discontinuity decreases to 0.9536 for $z = 2.0$ and is shown by the brown curve in Figure 11. Figures 7 – 10 show that there are following jumps at $z = 2.0$ for viscosity ratio $\frac{\overline{\eta}}{\overline{\mu}} = 2$ and at $z = 3.0$ for the viscosity ratio $\frac{\overline{\eta}}{\overline{\mu}} = 5$ when the z effective is bigger than one. These figures also show that the subsequent jumps for each ratio of viscosity parameters are getting smaller as time increases. However, Figures 5 and 6 show that the discontinuities are so small that the velocity graphs appear to be increasing smoothly to a horizontal asymptote at $v = 1$. Actually there are jumps according to the viscoelastic discontinuity analysis. Since the numerical values are very small compared to the other jumps, they are not apparent in the results.

For bigger viscosity time constants which are displayed in Figures 9 and 10, the velocity curves remain constant in between two discontinuity jumps. However when the viscosity time constants are $\overline{\eta} = 5$, $\overline{\eta} = 2$ and $\overline{\mu} = 1$, the velocity curves show a linear increase between two discontinuity jumps. Furthermore Figures 5 and 6 show that the velocity curves are increasing smoothly until the curves settle down as the velocities approach one.

This effect is also shown in Figures 12 and 13 where, as the viscosity time constants increase, the velocity curves also increase with different trends. In Figure 12 for $z = 0.333$, the green curve, which represents the velocity when the viscosity time constants are $\overline{\eta} = 0.5$ and $\overline{\mu} = 0.1$, increases smoothly compared to the velocity curves for viscosity time constants $\overline{\eta} = 5$ and $\overline{\mu} = 1$ and $\overline{\eta} = 50$ and $\overline{\mu} = 10$ which are represented by the blue and red curves respectively. There is an increment in the blue curve between $t = \alpha\sqrt{\frac{\overline{\mu}}{\overline{\eta}}}$ and $t = 3\alpha\sqrt{\frac{\overline{\mu}}{\overline{\eta}}}$ or before the arrival of the second wave. These increments continue to appear in the velocity curve before the arrival of the next waves. However, for the red curve the velocity is constant between $t = \alpha\sqrt{\frac{\overline{\mu}}{\overline{\eta}}}$ and $t = 3\alpha\sqrt{\frac{\overline{\mu}}{\overline{\eta}}}$ or before the arrival of the second and subsequent waves. The same trend of results also appears for the ratio of acoustic impedance $\frac{\overline{\eta}}{\overline{\mu}} = 2$, when $z = 1.2$ in Figure 13. Since $z = 1.2$ or z effective $\left(z^* = z\sqrt{\frac{\overline{\mu}}{\overline{\eta}}}\right)$, $z^* = 0.849$ is closed to 1 for the ratio of viscosity time constants $\frac{\overline{\eta}}{\overline{\mu}} = 2$, the following subsequent jumps are not apparent here. This trend of result is also shown in Figures 7 and 9 when $z = 1.5$ or $z^* = 1.06$. Another significant finding shown by Figures 12 and 13 is that the jumps are bigger for large viscosity time constants. Figure 12 shows that the first discontinuity is 0.37 (Blue curve) when the viscosity time constants are $\overline{\eta} = 5$ and $\overline{\mu} = 1$ and when the

viscosity time constants are $\overline{\eta} = 50$ and $\overline{\mu} = 10$, the first discontinuity is 0.45 (blue curve). Moreover Figure 13 shows the first discontinuity is 0.85 (Blue curve) for viscosity time constants $\overline{\eta} = 2$ and $\overline{\mu} = 1$ and 0.98 (red curve) when viscosity time constants are $\overline{\eta} = 20$ and $\overline{\mu} = 10$.

The discussion shows that the effective ratios of acoustic impedance z^* and the viscosity time constants $\overline{\eta}$ and $\overline{\mu}$ play a very important role in determining the behaviours of the wave transmitted through the viscoelastic slug.

Table 1. Predicted velocity discontinuities obtained using viscoelastic discontinuity analysis

z	$\overline{\eta}$	$\overline{\mu}$	z^*	$1stP_{JVD}$	$2ndP_{JVD}$	z	$\overline{\eta}$	$\overline{\mu}$	z^*	$1stP_{JVD}$	$2ndP_{JVD}$
0.333	0.2	0.1	0.235	0.1053	0.00118	0.333	0.5	0.1	0.149	0.0754	0.00116
0.667			0.472	0.1487	0.000559	0.667			0.298	0.1183	0.000966
0.9			0.636	0.1623	0.000233	0.9			0.402	0.1368	0.000693
1.2			0.849	0.1696	0.0000332	1.2			0.537	0.1520	0.000387
1.5			1.061	0.1706	0.00000431	2.5			1.118	0.1666	0.0000174
2.0			1.414	0.1657	0.000142	3.0			1.342	0.1636	0.0000973
0.333	2	1	0.235	0.5171	0.139	0.333	5	1	0.149	0.3773	0.145
0.667			0.472	0.7299	0.0660	0.667			0.298	0.5919	0.121
0.9			0.636	0.7966	0.0276	0.9			0.402	0.6844	0.0868
1.2			0.849	0.8323	0.00392	1.2			0.537	0.7602	0.0483
1.5			1.061	0.8372	0.000509	2.5			1.118	0.8336	0.00181
2.0			1.414	0.8133	0.0168	3.0			1.342	0.8184	0.0122
0.333	20	10	0.235	0.6062	0.224	0.333	50	10	0.149	0.4433	0.235
0.667			0.472	0.8558	0.106	0.667			0.298	0.6953	0.196
0.9			0.636	0.9340	0.0445	0.9			0.402	0.8040	0.141
1.2			0.849	0.9759	0.00636	1.2			0.537	0.8930	0.0783
1.5			1.061	0.9816	0.000821	2.5			1.118	0.9792	0.00758
2.0			1.414	0.9536	0.0271	3.0			1.342	0.9614	0.0197

$1stP_{JVD}$ is predicted velocity discontinuities at the interface $X = 1$, for $\alpha = 1$ and $t = \sqrt{\frac{\overline{\mu}}{\overline{\eta}}}$.

$2ndP_{JVD}$ is predicted velocity discontinuities at the interface $X = 1$, for $\alpha = 1$ and $t = 3\sqrt{\frac{\overline{\mu}}{\overline{\eta}}}$.

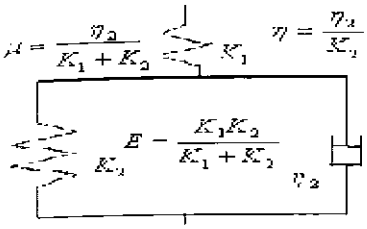

Figure 1: Standard Linear Solid Model

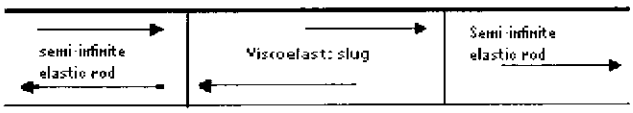

Figure 2: Wave movements in the rods and slug

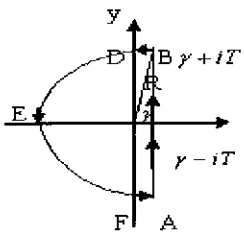

Figure 3: The Bromwich Contour

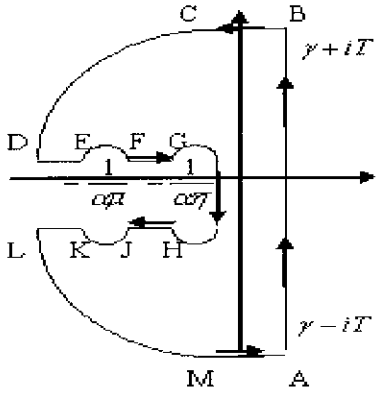

Figure 4: Closed Contour χ

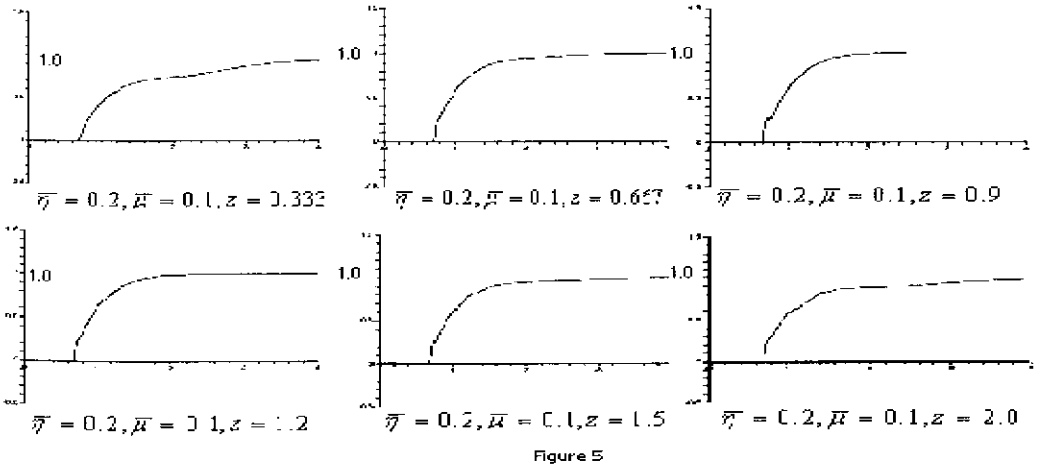

Figure 5: Particle velocity in the second rod at the interface $X = 1$ for $\bar{\eta} = 0.2$ and $\bar{\mu} = 0.1$

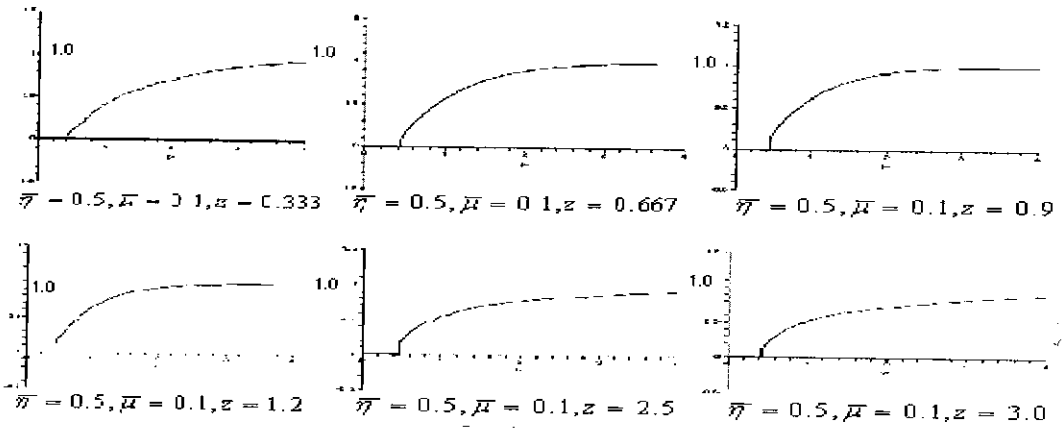

Figure 6: Particle velocity in the second rod at the interface $X = 1$ for $\bar{\eta} = 0.5$ and

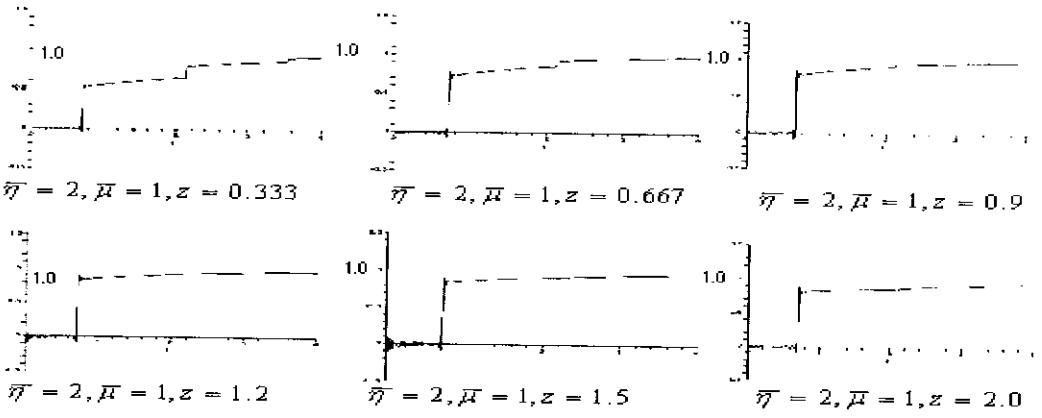

Figure 7: Particle velocity in the second rod at the interface $X = 1$ for

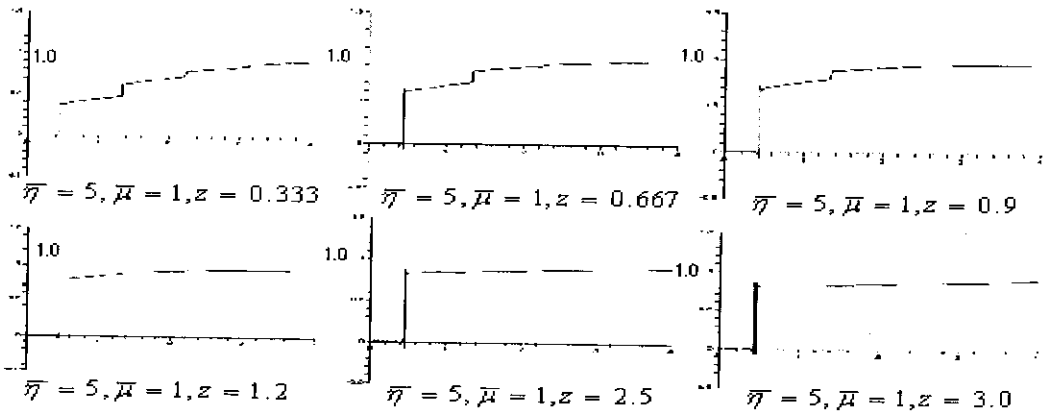

Figure 8: Particle velocity in the second rod at the interface $X = 1$ for $\bar{\eta} = 5$ and $\bar{\mu} = 1$

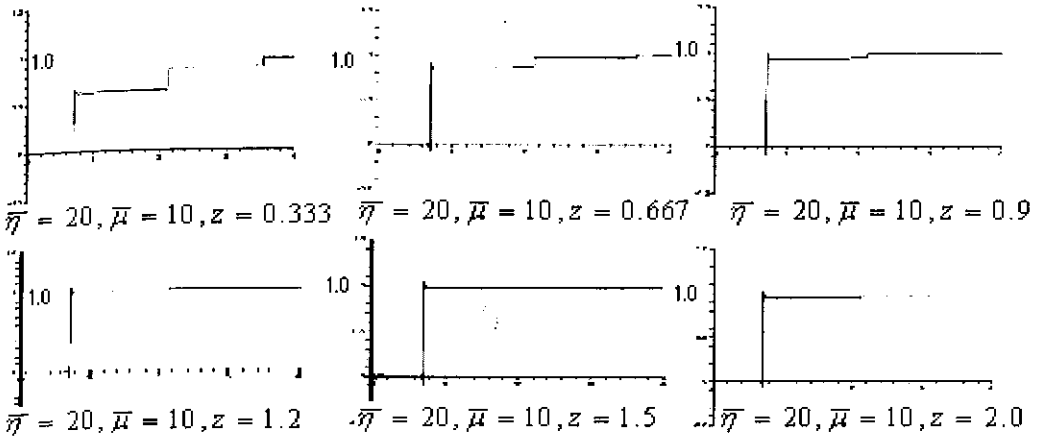

Figure 9: Particle velocity in the second rod at the interface $x = 1$ for $\overline{\eta} = 20$ and $\overline{\mu} = 10$

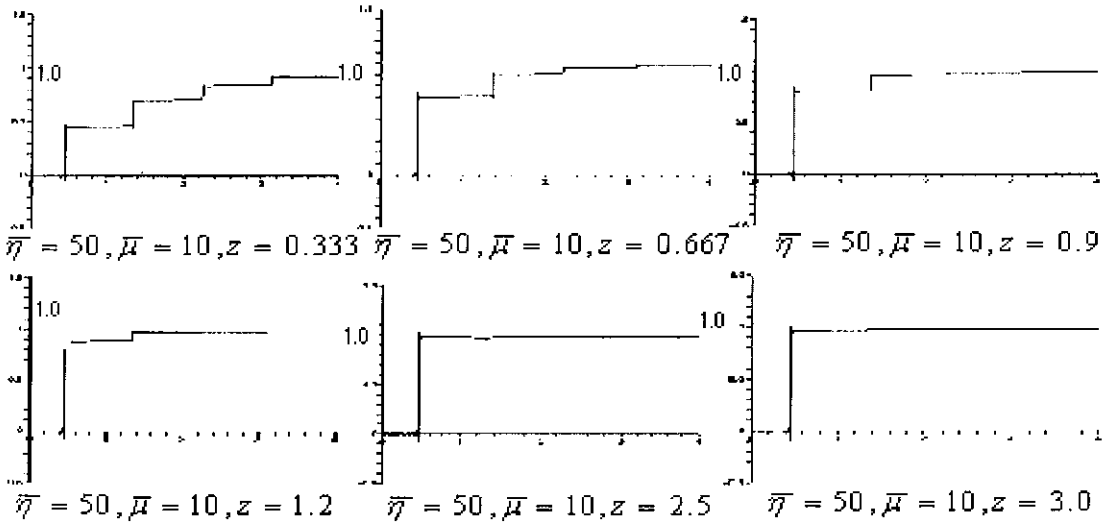

Figure 10: Particle velocity in the second rod at the interface $x = 1$ for $\overline{\eta} = 50$ and $\overline{\mu} = 10$

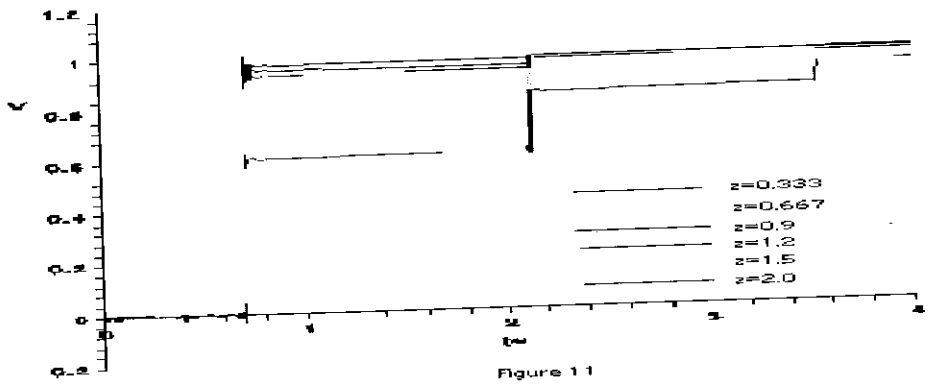

Figure 11: Velocity discontinuities in the second rod at the interface $X=1$ for $\bar{\eta}=20$ and $\bar{\mu}=10$

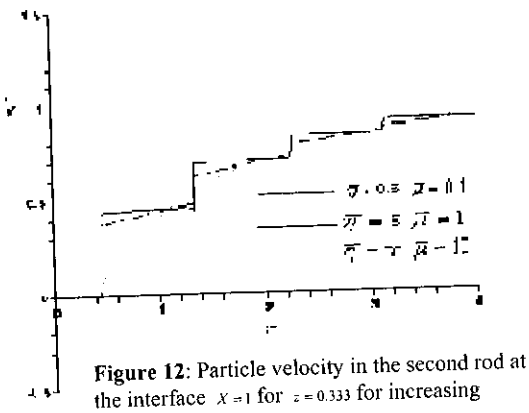

Figure 12: Particle velocity in the second rod at the interface $X=1$ for $z=0.333$ for increasing viscosity parameter ratio of $\frac{\bar{\eta}}{\bar{\mu}}=5$

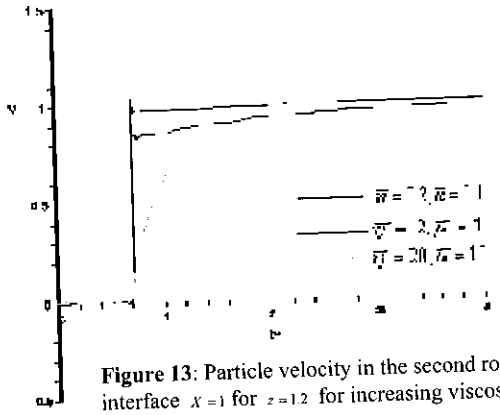

Figure 13: Particle velocity in the second rod at the interface $X=1$ for $z=1.2$ for increasing viscosity parameter ratio of $\frac{\bar{\eta}}{\bar{\mu}}=2$

REFERENCES

1. Christensen, R.M. (1971). *Theory of Viscoelasticity: An Introduction.* First edition, Academic Press.
2. Bland, D.R. (1960). *The Theory of Linear Viscoelasticity.* International Series of Monographs on Pure and Appl. Math.. Pergamon Press.
3. Kolsky, H. (1963). *Stress Waves in Solids.* First edition, Dover Publication.
4. Kolsky, H. (1949). An Investigation of the Mechanical Properties of Materials at Very High Rates of Loading. *Proc. Phys. Soc. London.* **B62**: 676.
5. Stronge, W.J. (2000). *Impact Mechanics.* Cambridge University Press, Cambridge, United Kingdom.
6. Spiegel, M.R. (1983). *Advanced Mathematics For Engineers and Scientist.* Schaum's Outline Series, McGraw-Hill Book Co. Singapore.
7. Musa, A.B. (2005). *Wave Motion and Impact Effects in Viscoelastic Rods.* PhD thesis, Loughborough University, England.
8. Musa, A.B. (2006). *Viscoelastic Discontinuity Analysis for Wave Propagation in Viscolestic slug.* EDU Research-UPSI, Kuala Lumpur.
9. Nayfeh, A.H. (1993). *Introduction to Perturbation Techniques.* Library edition, John Wiley & Sons, Inc.: 28-38.